Available online at www.sciencedirect.com
SCIENCE DIRECT
Journal of Catalysis 233 (2005) 317–326
JOURNAL OF CATALYSIS
www.elsevier.com/locate/jcat

Decomposition of methane with an autocatalytically reduced nickel catalyst

Richard A. Couttenye [a], Marianela Hoz De Vila [a], Steven L. Suib [a,b,c,*]

[a] *Department of Chemical Engineering, University of Connecticut, Storrs, CT 06269-3222, USA*
[b] *Institute of Material Science, University of Connecticut, Storrs, CT 06269-3136, USA*
[c] *Department of Chemistry, University of Connecticut, Storrs, CT 06269-3060, USA*

Received 4 March 2005; revised 5 May 2005; accepted 10 May 2005

Available online 6 June 2005

Abstract

Thermal decomposition of nickel acetate ($T > 300\,^{\circ}C$) dispersed on either silica or cordierite supports resulted in a mixture of Ni^0/NiO that was catalytically active for the decomposition of methane to produce CO-free hydrogen, without the need for any pretreatment (i.e., using H_2 at high temperature ($> 500\,^{\circ}C$) for at least 2 h). The carbon yield (g_C/g_{Ni}) for the catalysts supported on SiO_2 ($\sim$ 200–300 m^2/g) increased with an increase in the catalyst NiO mean crystallite size. XRD and FE-SEM studies confirmed the formation of graphitic-type carbon filaments during the methane decomposition.

Keywords: Hydrogen production; Methane decomposition; Nickel acetate

1. Introduction

The search for alternative energy sources has been propelled by the reduction of petroleum reserves around the world and by pollution caused by the increase in energy consumption. Compared with other options, such as solar or wind energy, the use of hydrogen (H_2) to satisfy future energy demand emerges as an attractive choice. Hydrogen, a clean-burning fuel, has been widely used in petroleum refineries, the production of ammonia, the hydrogenation of fats and oils, welding, the production of hydrochloric acid, the electronics industry, fuels for rockets, and recently in fuel cells. Worldwide, 48% of H_2 is produced from natural gas, 30% from petroleum (mostly consumed in refineries), 18% from coal, and the remaining 4% from water electrolysis [1].

Electrolytic production of H_2, a highly inefficient process, is only attractive when low-cost hydroelectric power is available [1]. In addition, technologies for hydrogen generation from biomass, such as enzymatic decomposition of sugars, steam reforming of bio-oils, and gasification, suffer from low production rates and/or complex processing requirements [2].

In contrast, decomposition of methane over supported metal catalysts (preferably nickel) [3–15] produces very pure H_2 without the formation of carbon oxides, which eliminates the process of separating the gaseous mixtures. However, such an advantage is outweighed by the catalyst deactivation due to carbon deposition on the active sites, hence requiring regeneration by conventional oxidation in air or steam gasification [3,4,11]. Catalytic decomposition of methane is therefore a useful application in some specific cases, such as hydrogen fuel cells (e.g., proton-exchange membrane, PEM), where CO-free hydrogen is required to avoid deactivation of the platinum electrode.

Nickel has been the most common transition metal used for decomposition, steam reforming, and/or partial oxidation of methane. For instance, Amiridis et al. [3,4] have been using 15% Ni/SiO_2 for the decomposition of methane to produce CO-free hydrogen, and have found that fila-

* Corresponding author. Fax: +1 860 486 2981.
E-mail address: suib@uconnvm.uconn.edu (S.L. Suib).

0021-9517/$ – see front matter
doi:10.1016/j.jcat.2005.05.006

mentous carbon started to grow when attached to a nickel crystallite, which eventually led to catalyst deactivation. Dicks [5], Matsukata [6], and Ermakova [7] have also reported the formation of filamentous carbon during the decomposition of methane with the use of 5% Ni/SiO_2 and 90–96% nickel with different textural promoters (SiO_2, Al_2O_3, MgO, TiO_2, and ZrO_2). Froment et al. have comprehensively studied the filamentous carbon formation and the gasification process during methane decomposition [8]. Takenaka et al. [9,10] have used 40% Ni/SiO_2 and 37% (Pd–Ni)/carbon nanofibers to decompose methane into hydrogen, attaining the highest hydrogen yield among those reported yet (16,000 $mol_{H_2}/mol_{(Pd+Ni)}$), for the mixture 37% (Pd–Ni) supported on carbon nanofibers. Choudhary et al. [11–13] have studied the continuous production of H_2 from methane decomposition over Ni-containing metal-oxide (Ni/M = 1.0) and nickel (10%)-impregnated zeolite and SiO_2 catalysts. Gronchi [14] synthesized nickel-supported catalysts on SiO_2 and Al_2O_3 in the form of xerogels, and the influence of surface differences on the catalytic activity of the materials was studied with the CH_4 reforming reaction. An extensive review of the multiple roles of catalysis in the production of hydrogen was made by Armor [1]. Armor highlights the use of nickel catalyst (∼ 12–20% nickel) supported on a refractory material, such as alpha alumina for steam reforming of methane. Recupero et al. [15] also used commercial Ni/Al_2O_3 (CRG-F) for steam reforming of methane.

However, nickel nitrate has been the preferred nickel salt in all of these studies. The thermal decomposition of nickel nitrate ($T > 400\,^{\circ}C$) produces nickel oxide (NiO). To reduce the nickel from oxide to nickel metal, pretreatment of the catalysts is required (with H_2 at high temperature ($> 500\,^{\circ}C$) for at least 2 h). On the other hand, many research studies [16–24] have characterized in detail the thermal decomposition of nickel acetate ($Ni(CH_3COO)_2{\cdot}4H_2O$). There is agreement [21,23,24] that this salt decomposes at temperatures higher than 250 °C through an autocatalytic process in which a nickel carbide (Ni_3C) intermediate species is formed. At temperatures higher than 300 °C, Ni_3C decomposes completely, giving rise to a mixture of Ni^0 and NiO.

To the best of our knowledge, the use of this peculiar mixture Ni^0/NiO from an acetate salt for catalytic purposes (such as the decomposition of methane) has not yet been reported. The present investigation evaluated the application of the Ni^0/NiO mixture, which was obtained after thermal decomposition of nickel acetate, for CO-free hydrogen production by means of decomposition of methane, with the use of two types of supports: cordierite monolith and SiO_2. Catalyst preparation, characterization, and catalytic performance were reported. The relationship between nickel oxide (NiO) mean crystallite sizes and catalyst deactivation, due to carbon deposition, was also studied.

2. Experimental

2.1. Catalyst preparation

2.1.1. Type 1

Celcor cordierite ($Mg_2Al_4Si_5O_{18}$) monoliths (as received) from Corning with square channels and a density of 400 squares/in^2 were cut into smaller pieces ($L = 20$ mm, $D = 9$ mm) and dipped in a 0.5 M aqueous solution of nickel(II) acetate tetrahydrate ($Ni(CH_3COO)_2{\cdot}4H_2O$, CAS: 6018-89-9; Aldrich Chemical Company, Milwaukee, WI) or nickelous nitrate hexahydrate ($Ni(NO_3)_2{\cdot}6H_2O$; JT Baker, Phillipsburg, NJ) for 3 h at room temperature and dried overnight in air at 120 °C. The monoliths were then calcined in air at 600 °C for 2 h. The final nickel content on the monoliths was 8 wt%. The samples were denoted Cor-A-8 and Cor-N-8, respectively (i.e., support–salt–wt%) (A = acetate, N = nitrate).

2.1.2. Type 2

Nickel catalyst supported on SiO_2 (Davisil 35-60 mesh, grade 646, type 150 A, Fisher) was prepared by conventional wet impregnation with a nominal metal loading of 8 and 40 wt%. Nickel(II) acetate tetrahydrate ($Ni(CH_3COO)_2{\cdot}4H_2O$, CAS # 6018-89-9; Aldrich Chemical Company, Milwaukee, WI) and nickelous nitrate hexahydrate ($Ni(NO_3)_2{\cdot}6H_2O$; JT Baker, Phillipsburg, NJ) were used as a source of nickel. After impregnation at room temperature, the catalysts were dried overnight at 120 °C and then calcined, in air, at 600 °C for 2 h. These samples were denoted Si-A-8, Si-A-40, Si-N-8, and Si-N-40, respectively.

2.2. X-ray diffraction

X-ray diffraction (XRD) analysis was used to identify the nature of the powder catalyst. XRD data were collected with a Scintag 2000 XDS diffractometer with Cu-K_α X-ray radiation. Powder samples were placed on aluminum slides and scanned at 4° 2θ/min. The beam voltage and beam current were 45 kV and 40 mA, respectively.

2.3. Scanning electron microscopy and field emission scanning electron microscopy

The morphology of the catalyst, before and after reaction, was recorded by scanning electron microscopy (SEM) and field emission scanning electron microscopy (FE-SEM). SEM micrographs were taken with an Amray 1810 microscope, and high-resolution micrographs were taken with a Zeiss DSM982 Gemini FE-SEM microscope. Samples were mounted on carbon tape onto aluminum sample holders for analysis.

2.4. Textural properties

The catalyst (types 1 and 2, as prepared) surface areas were measured, with the use of nitrogen physisorption

at liquid nitrogen temperature with a Micrometrics ASAP 2010 System. Before the analysis samples were outgassed at 300 °C under vacuum for 2 h. Surface areas were determined by nitrogen adsorption data, with Brunauer–Emmett–Teller (BET) methods.

2.5. Catalytic activity

Types 1 and 2 catalysts were tested for the decomposition of methane with a gas-flow quartz tube reactor (i.d. = 10 mm, length = 30 cm), operating at atmospheric pressure. The reactor was kept in a tubular electric furnace controlled by an Omega-4002A temperature controller, connected to a thermocouple placed at the center of the reactor. Methane (99% [Airgas]) was fed to the reactor at 40 ml/min and regulated by a MKS-247C flow controller. The catalysts (type 1: ∼ 0.6 g, or type 2: ∼ 0.040 g) were placed 17 cm from the reactor entrance with quartz wool to set up the catalyst bed. The gap between the catalytic bed and the reactor entrance was filled with glass beads (4 mm, cat # 11-312B; Fisher) in order to increase the contact area for preheating of the feed. Before the reaction started, the catalysts prepared with $Ni(NO_3)_2{\cdot}6H_2O$ as the nickel precursor were reduced with pure hydrogen at 550 °C for 2 h, unless otherwise mentioned. During the reaction, the product stream was analyzed by mass spectrometry (MS) with a MKS-UTI PPT quadrupole residual gas analyzer. The MS was calibrated before the experiments with the use of gaseous mixtures of H_2 in CH_4 of known concentrations: 5, 10, 15, 20, and 40%. Since CH_4 decomposition on nickel catalysts proceeds selectively to carbon and H_2 [3,7,9,10], methane conversion was calculated from the hydrogen concentration in the product mixture. The amount of carbon deposited on the catalyst during reaction was calculated by the weight difference from the fresh sample. Each experiment was performed three times with catalysts prepared in different batches (B1–B2–B3).

3. Results and discussion

3.1. Influence of nickel precursor on catalyst surface area and activity

Table 1 summarized the effect of the nickel precursor and type of support on the catalyst surface area. $Ni(CH_3COO)_2{\cdot}4H_2O$ was used as the nickel precursor and led to materials with higher surface areas than those obtained when $Ni(NO_3)_2{\cdot}6H_2O$ was used, regardless of the type of catalyst (1 or 2), as indicated in Table 1. In addition, the amount of nickel (wt%) used had an inverse effect on the catalyst surface area—the higher the Ni wt%, the lower the surface area. The difference in surface area between catalysts of types 1 and 2 was attributed to the catalyst support characteristic, since cordierite had a lower surface area (> 0.2 m^2/g) compared with that of SiO_2 (∼ 300 m^2/g).

Table 1
Effect of nickel precursor and support on catalysts surface area

Catalyst[a]	Nickel precursor	Nickel (wt%)	BET surface area (m^2/g)		
			B1	B2	B3
Type 1					
Cor-A-8	$Ni(CH_3COO)_2{\cdot}4H_2O$	8	5.8	6.3	5.1
Cor-N-8	$Ni(NO_3)_2{\cdot}6H_2O$	8	2.9	2.1	3.4
Type 2					
Si-N-40	$Ni(NO_3)_2{\cdot}6H_2O$	40	178.5	169.8	173.1
Si-A-40	$Ni(CH_3COO)_2{\cdot}4H_2O$	40	249.8	230.2	255.7
Si-N-8	$Ni(NO_3)_2{\cdot}6H_2O$	8	273.4	277.2	266.4
Si-A-8	$Ni(CH_3COO)_2{\cdot}4H_2O$	8	285.5	294.6	280.8

[a] Sample nomenclature: support–salt–wt%.

The changes in methane conversion with time during the catalytic decomposition of methane at 550 °C, with types 1 and 2 catalysts (from batch B1), are shown in Fig. 1. At the beginning of the reaction, the catalysts containing 40 wt% nickel resulted in higher conversion (13–15%) than the catalysts with 8 wt% nickel loading (7–10%). However, the initial activity of the catalyst prepared with nickel acetate, without reduction pretreatment (Fig. 1, curves 2, 6, and 7), was very close to the initial activity obtained with the catalysts that were prepared with nickel nitrate and pre-reduced with H_2 at 550 °C for 2 h (Fig. 1, curves 1, 4, 5). The conversion data for the unreduced Si-N-40 catalyst are also included in Fig. 1 (curve 3). Clearly, the conversion of methane with this unreduced catalyst was lower than that obtained with the pre-reduced Si-N-40 (Fig. 1, curve 1). This difference in activity illustrated the reduction effect on the catalysts prepared from the nitrate salt and the advantage of using nickel acetate as a precursor (reduction free).

3.2. XRD characterization

Decomposition of nickel(II) acetate tetrahydrate ($Ni(CH_3COO)_2{\cdot}4H_2O$) in air at 600 °C for 2 h resulted in the formation of a mixture of Ni^0/NiO, as indicated by the XRD pattern shown in Fig. 2a (Ni^0: $2\theta = 43.7°$, 51.1°, 75.6° JCPDS # 4-850; NiO: $2\theta = 36.4°$, 42.5°, 62.0°, 78.6° JCPDS # 4-835). Thermal decomposition of nickelous nitrate hexahydrate ($Ni(NO_3)_2{\cdot}6H_2O$) in air at 600 °C for 2 h resulted in the formation of NiO, as shown in Fig. 2b (NiO: $2\theta = 36.4°$, 42.5°, 62.0°, 78.6° JCPDS # 4-835). However, when the nickel precursors (acetate, nitrate) were impregnated on SiO_2 or cordierite and calcined in air at 600 °C for 2 h, the main product detected by XRD was NiO, regardless of the percentage weight of nickel, as indicated in Fig. 3 (a–d) and Fig. 4b. In contrast, Fig. 3 (e and f) shows that the oxidation state of nickel changed after reaction with methane; that is, the NiO present in the catalysts Si-A-40 and Si-N-40 (without H_2 pretreatment) was reduced to Ni^0. The same observation was valid for the Cor-A-8 (Fig. 4c) after reaction with methane.

The difference in relative intensity of the carbon peak (graphitic-type [3] $2\theta = 26.1°$ (strongest), and $2\theta = 42.6°$,

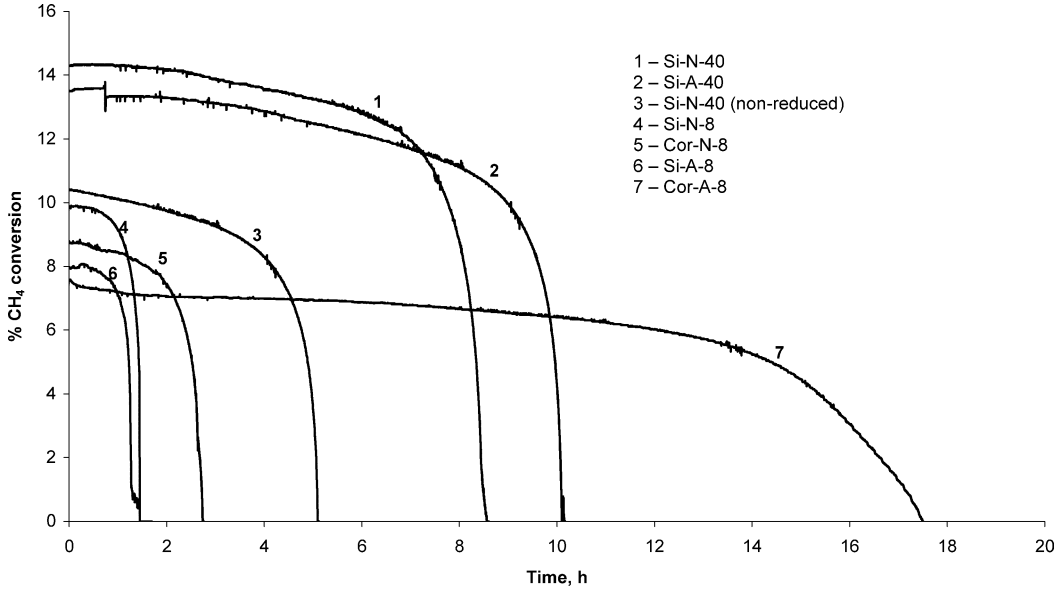

Fig. 1. Changes in methane conversion during methane decomposition using B1 nickel catalysts. Experimental conditions: temperature = 550 °C, pressure = 1 atm, and flow rate = 40 ml/min.

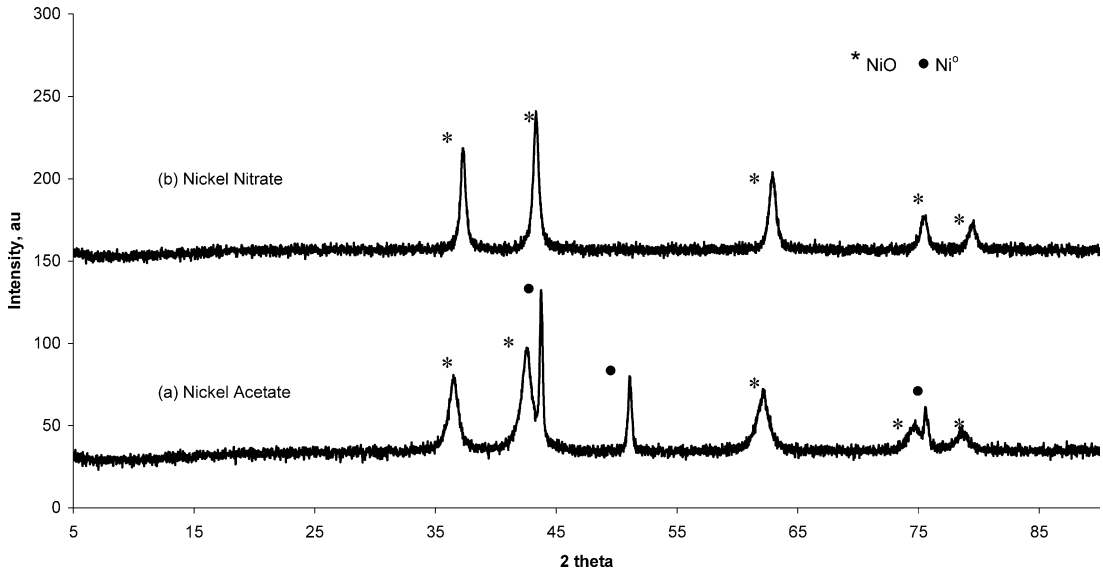

Fig. 2. XRD patterns of (a) nickel acetate, and (b) nickel nitrate, after decomposition in air at 600 °C during 2 h.

53.8°, 77.6°) with respect to the Ni^0 peaks, between the sample Si-A-40 and Si-N-40 (see Fig. 3, e and f), was higher for the catalyst prepared with the acetate precursor, thus indicating that a larger amount of carbon was deposited on this catalyst; that is, the catalyst Si-A-40 had higher activity in the decomposition of methane than Si-N-40 (as prepared). Fig. 5A shows the XRD pattern for the catalyst Si-A-40 after complete deactivation (10-h reaction with methane). The change in relative intensity of the carbon peak with respect to the Ni^0 peaks indicated that an additional amount of carbon was accumulated on the catalyst as the reaction proceeded.

Steam regeneration [3,4,11] of the catalyst was performed with a 50% steam in He mixture at 600 °C. After the regeneration process, the catalyst preserved its metallic nickel form; however, some NiO appeared because of overexposure to steam [4] (see Fig. 5B). Under the experimental conditions small amounts of carbon also resisted gasification. The XRD pattern of the regenerated catalyst after subsequent methane decomposition at 550 °C (Fig. 5C) shows that nickel was in metallic form (Ni^0) and carbon (graphitic-type) was again deposited on the catalyst. The relative intensity of the carbon peak with respect to the Ni^0 peaks between the fresh and regenerated catalysts (Fig. 5, A and C) suggested that the activity of the regenerated catalyst was similar to the activity of the fresh catalyst. For instance, Amiridis et al. [4] indicated that 15 wt% Ni/SiO_2 catalysts showed no significant decrease in methane conversion, even after 10 cycles of methane decomposition–steam regeneration. The author

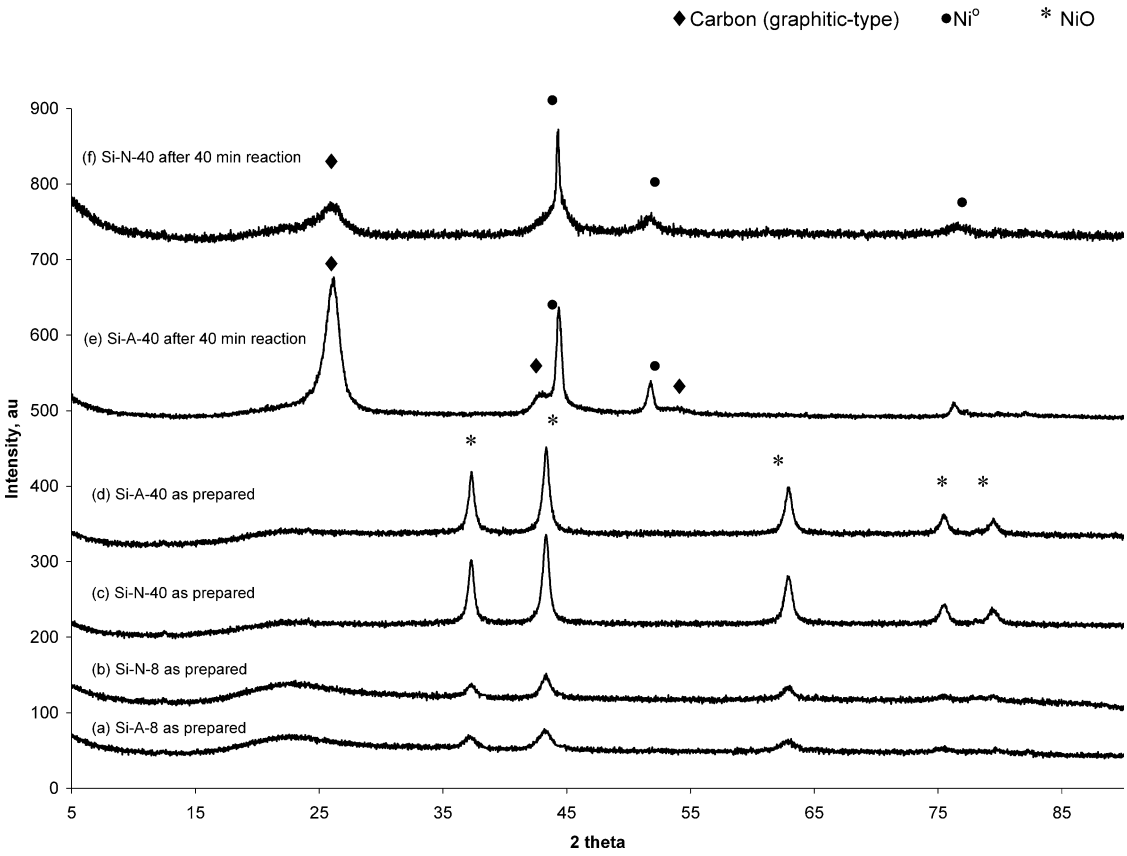

Fig. 3. XRD patterns of Ni/SiO_2 catalysts: (a–d) after calcination in air at 600 °C for 2 h, (e–f) after reaction with methane at 550 °C for 40 min.

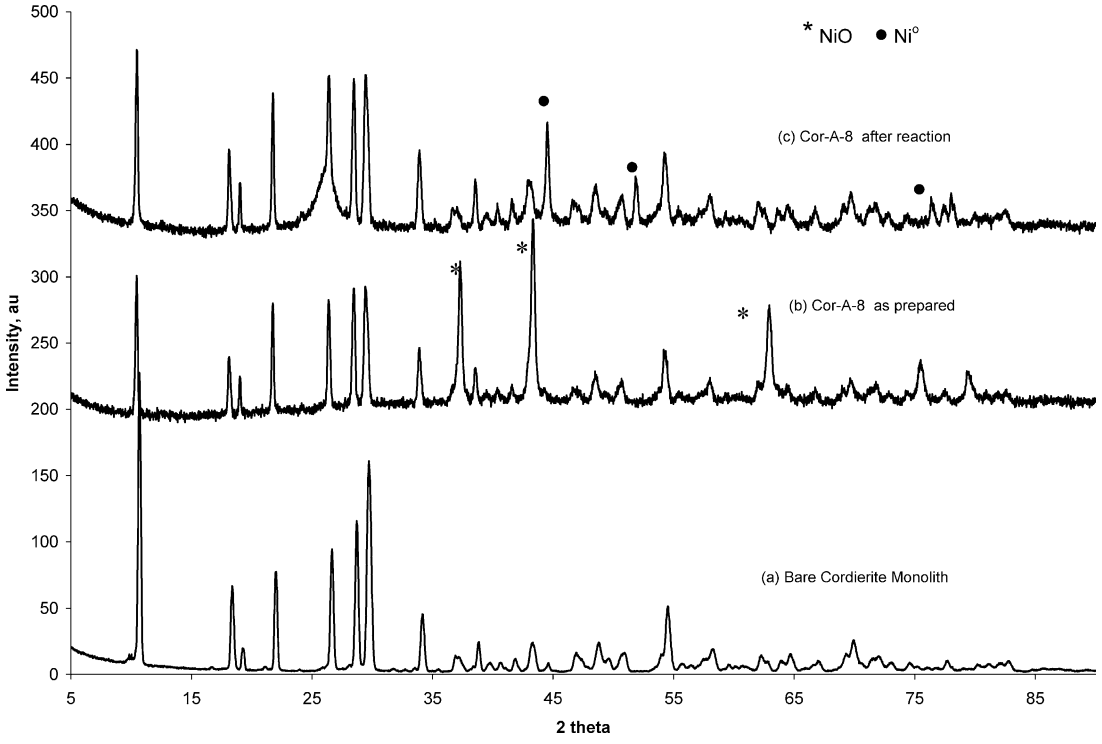

Fig. 4. XRD patterns of Ni/cordierite catalyst: (a) bare cordierite monolith, (b) after calcination in air at 600 °C for 2 h, and (c) after reaction with methane at 550 °C for 17 h.

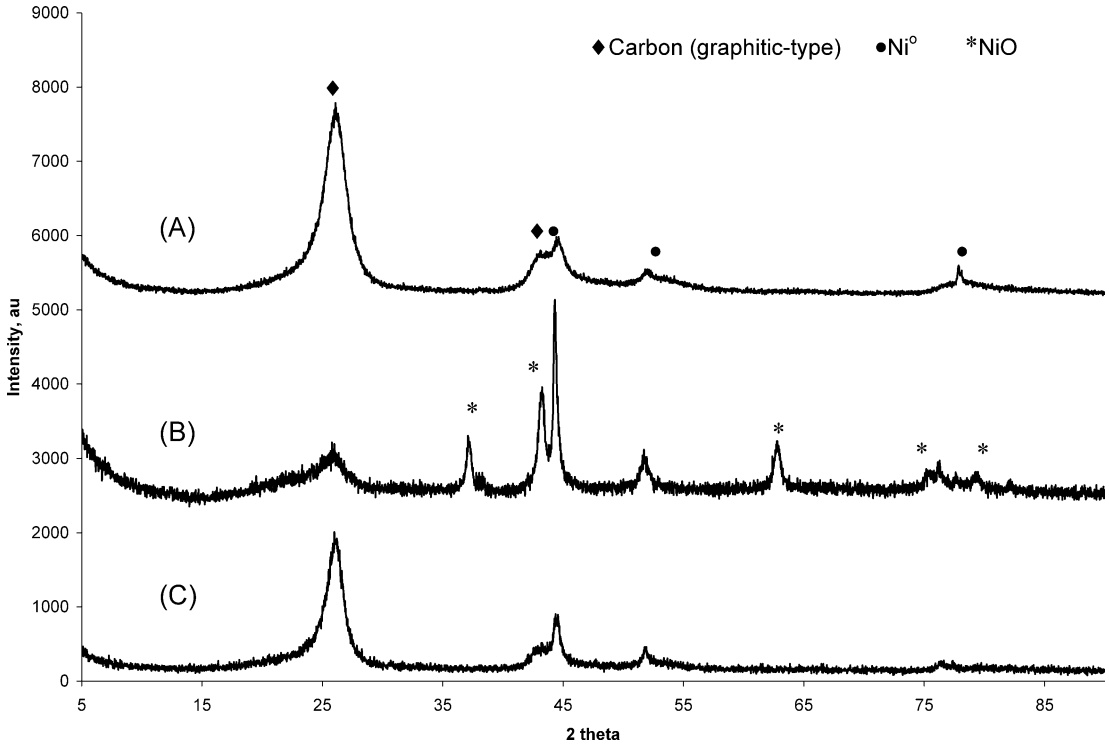

Fig. 5. XRD patterns of catalyst Si-A-40: (A) after reaction with methane at 550 °C for 10 h, (B) after steam regeneration at 600 °C for 10 h, (C) regenerated catalyst after subsequent methane decomposition at 550 °C for 10 h.

also highlighted the presence of small amounts of carbon after steam regeneration; however, in increase of this type of carbon was observed from cycle to cycle.

3.3. Mass spectrometry

Mass spectrometry analyses performed during the reaction with catalysts Si-A-40 and Si-N-40, without reduction pretreatment (Fig. 6, A and B), indicated the simultaneous formation of carbon monoxide (CO, $m/z = 28$) and carbon dioxide (CO_2, $m/z = 44$), immediately after exposure to methane, for ∼ 6 min (see Fig. 6, inset). The difference in partial pressure of CO and CO_2 between the two catalysts suggested that the initial amount of oxygen available, as NiO, was lower for Si-A-40 than the amount available for Si-N-40. It is known that nickel oxide (NiO) reacts slowly with methane (at 700 °C) to produce CO_2, H_2O, and, eventually, Ni^0 [25–27]. On the other hand, methane decomposes rapidly on Ni^0 to produce H_2 and carbon (adsorbed to the nickel surface). Adsorbed carbon reacts with NiO to form CO and Ni^0 [25,28]. Ni^0 could also catalyze the decomposition of CO to produce CO_2 and carbon (i.e., Boudouard reaction) [25]. Consequently, the immediate and simultaneous formation of CO and CO_2 at the beginning of the reaction indicated the presence of Ni^0 in Si-A-40 and Si-N-40 catalysts (as prepared), but with concentration below the XRD detection limit. After the in situ reduction of nickel, the only reaction products detected by mass spectrometry were H_2 and CH_4 (i.e., carbon oxides were not detected). For instance, Choudhary et al. [13] reported that the level of CO formed during methane decomposition was 50 ppm when they used 10 wt% Ni/SiO_2 catalysts.

Table 2
Catalysts carbon yield and NiO mean crystallite size

Catalyst[a]	Amount of catalyst used (g)			Mass of carbon deposited (g)			NiO mean crystallite size (Å)		
	B1	B2	B3	B1	B2	B3	B1	B2	B3
Type 1									
Cor-A-8	0.59	0.61	0.60	1.13	0.63	1.68	167	125	195
Type 2									
Si-A-40	0.044	0.047	0.041	1.35	1.60	1.12	182	200	160
Si-A-40[b]	0.040	0.040	0.040	0.87	0.93	0.98	49	56	62
Si-A-8	0.040	0.041	0.040	0.12	0.13	0.11	20	24	15

[a] Sample nomenclature: support–salt–wt%.
[b] Calcined in nitrogen at 600 °C for 2 h.

3.4. Effect of nickel oxide (NiO) mean crystallite size on catalyst carbon yield (g_C/g_{Ni})

Table 2 shows the NiO mean crystallite size estimated with the Sherrer equation, based on the half-width of the diffraction peaks assigned to [200] and [111] NiO, for the catalyst prepared with the acetate precursor. The experimental results listed in Table 2 suggest that the catalysts' NiO mean crystallite size was affected by (1) the nickel wt%, (2) the type of gas used during calcination (air or nitrogen), and (3) the catalyst support. The carbon yield (total mass of

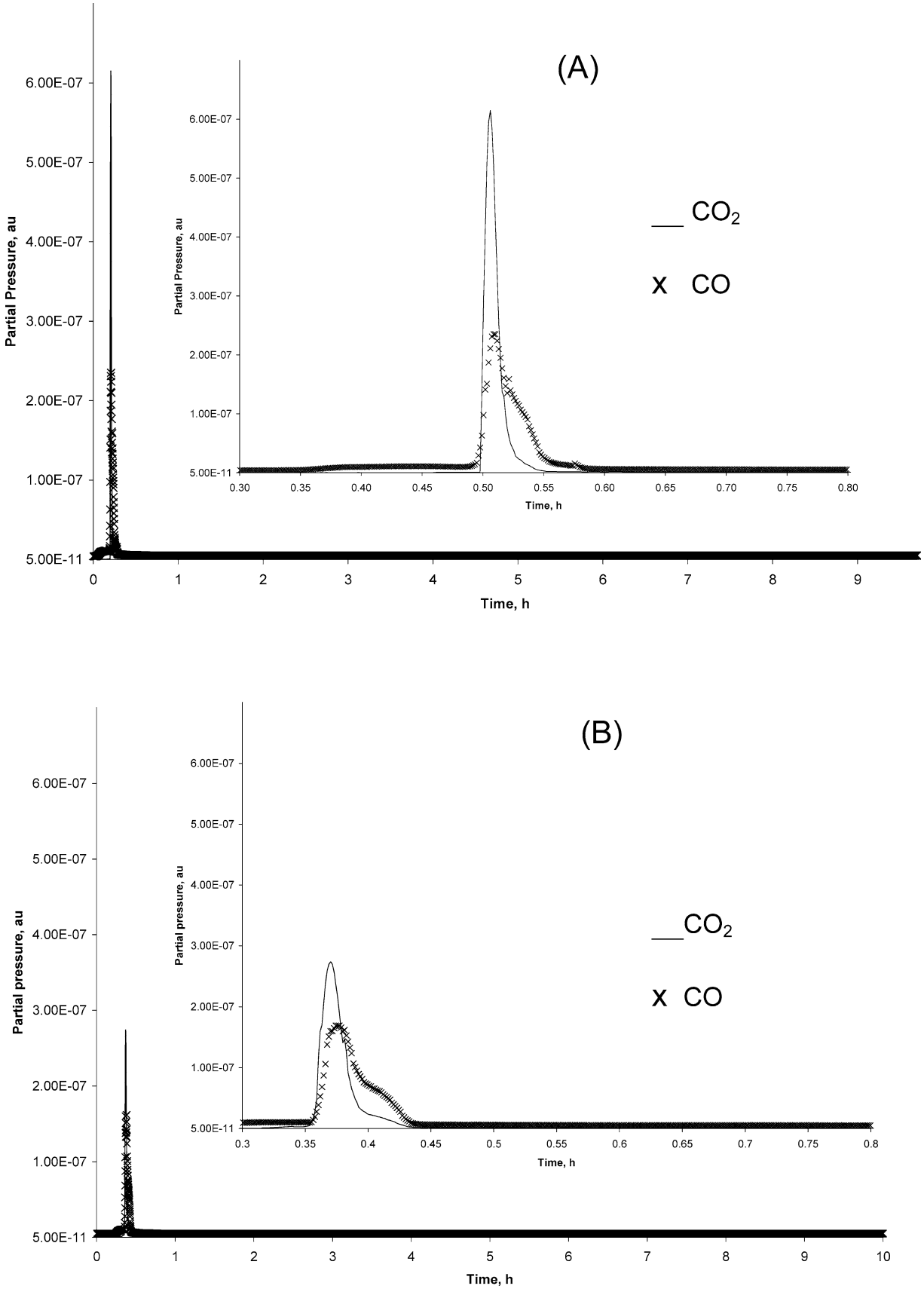

Fig. 6. Carbon monoxide (CO, $m/z = 28$), and carbon dioxide (CO_2, $m/z = 44$) production monitored by mass spectrometer during decomposition of methane at 550 °C, using samples: (A) Si-N-40 and (B) Si-A-40—without reduction pretreatment.

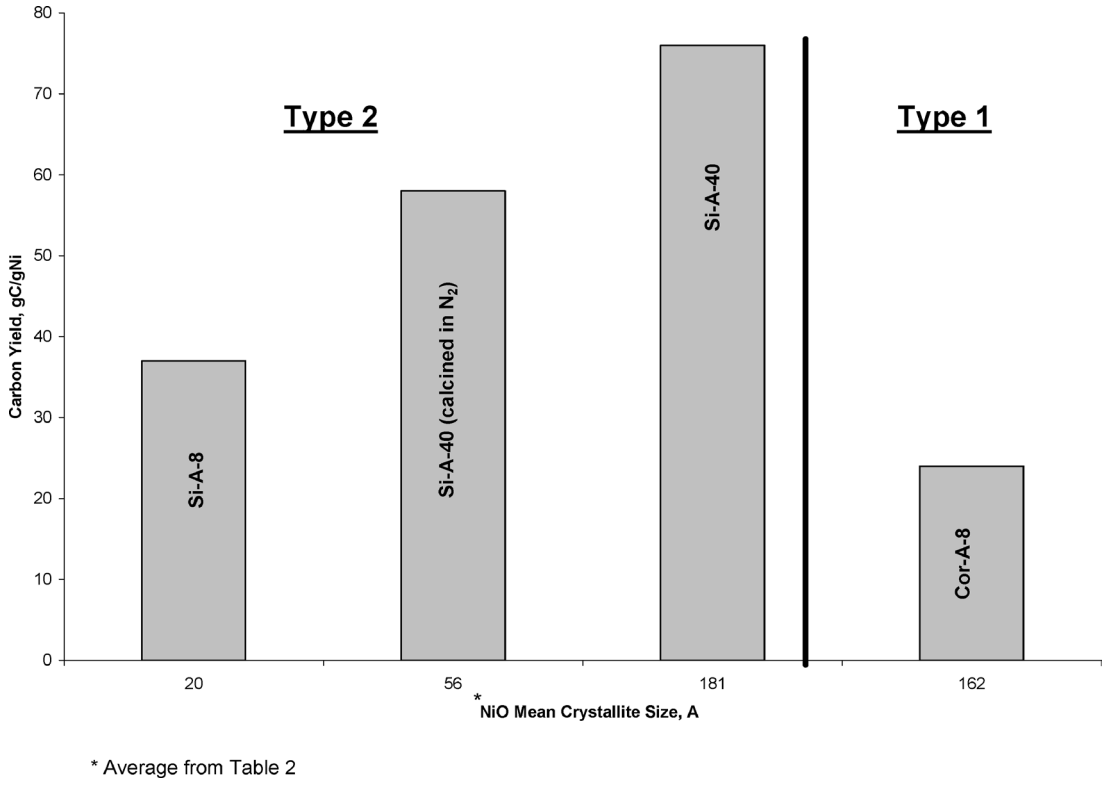

Fig. 7. Effect of NiO mean crystallite size on the catalysts carbon yield.

carbon (in grams) deposited on the catalyst after complete deactivation, divided by catalyst nickel mass (in grams)) is a common representation of the catalyst activity for decomposition of methane [7,9,10,29]. Fig. 7 shows the effect of NiO mean crystallite size on the catalyst carbon yield. For type 2 catalysts, as the NiO mean crystallite size increased, the carbon yield of the catalysts also increased (see Fig. 7). Calcination of sample Si-A-40, under nitrogen at 600 °C for 2 h, resulted in a catalyst with a smaller NiO mean crystallite size. Consequently, this catalyst had a lower carbon yield, despite having 40 wt%. Ermakova et al. [7] reported that the presence of SiO_2 (10 wt% or higher) stabilized NiO particles (with diameter < 65 nm) during reduction with H_2, and decreased sintering of the Ni^0 particles being formed. The author also indicated that as the diameter of the Ni^0 particle increased (10–40 nm), the carbon yield of the catalyst for decomposition of methane increased as well; however, a further increase in the size of Ni^0 particles above 40 nm resulted in a sharp decrease in carbon yield. Similarly, the experimental results shown in Fig. 7 for type 2 catalysts suggest that the presence of SiO_2 stabilized the NiO particles (diameter = 2–18 nm) and the Ni^0 particles (initially in the catalyst), minimizing the sintering during the in situ reduction of NiO by methane. For instance, the mean crystallite size of Ni^0 particles formed in the catalyst Si-A-40 after reaction with methane, for 10 h, was ~ 25 nm (estimated with the Sherrer equation based on half-width of the diffraction peaks assigned to (200), and (111) Ni^0). In addition, Fig. 7 showed that the carbon yield obtained with sample Si-A-8 was higher than the yield obtained with Cor-A-8, even though the NiO mean crystallite size was higher (~ 16 nm) for the catalyst prepared with cordierite (Cor-A-8). In this case, the mean crystallite size of Ni^0 particles formed in the catalyst Cor-A-8 after reaction with methane, for 17 h, was ~ 34 nm. This result suggested that cordierite could not stabilize the NiO or Ni^0 particles in the same way as SiO_2, and sintering of Ni^0 particles increased.

3.5. SEM and FE-SEM characterization

The micrograph of the spent Cor-A-8 catalyst (Fig. 8a) showed a moss-like material deposited on the catalyst surface. A high-magnification micrograph revealed the presence of nickel particles ($\sim$ 30–300 nm) located at the tip of carbon filaments (Fig. 8b). The formation of graphitic-type carbon filaments (as indicated by the increased intensity of the XRD peak at $2\theta = 26.1°$ (Fig. 4c) and FE-SEM (Fig. 8b)) suggested that the decomposition of methane with catalyst Cor-A-8 followed a mechanism similar to one proposed elsewhere [3,5–8]. In particular, these authors reported that carbon filament formation gave the catalyst the capability of accommodating a significantly higher amount of carbon than those predicted by either the site-blocking or pore-mouth plugging models. However, because of spatial limitations (i.e., loss of exposed nickel surface), the growth of carbon filaments was terminated, and the catalyst was deactivated.

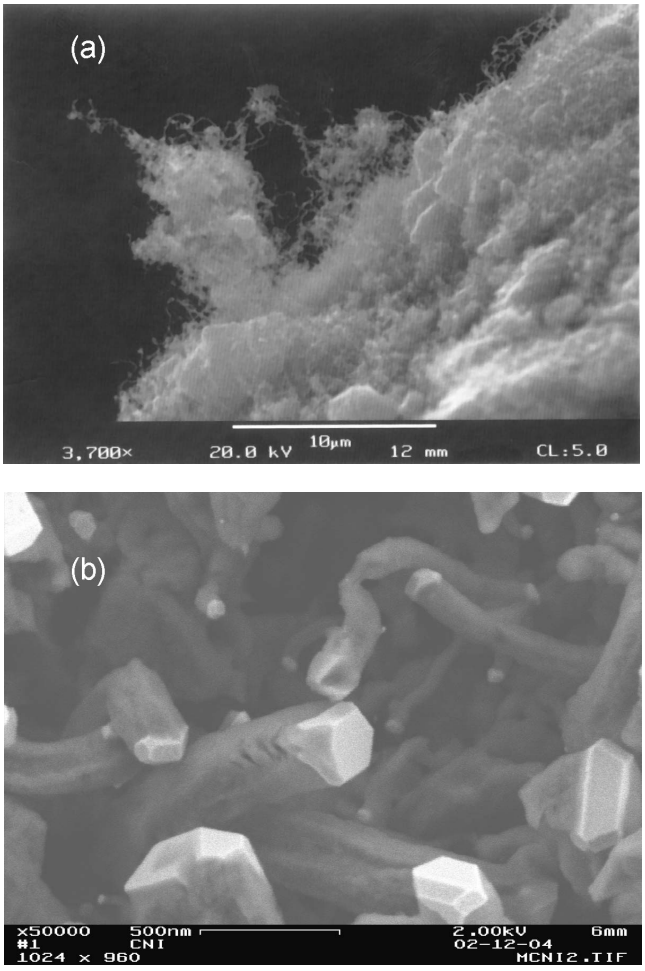

Fig. 8. (a) SEM micrograph, and (b) FE-SEM high-resolution micrograph, of Cor-A-8 catalyst after reaction with methane at 550 °C for 17 h.

4. Conclusions

Based on the results obtained, the following conclusions can be made:

(1) For the first time, the Ni^0/NiO mixture obtained by thermal decomposition of nickel acetate has been successfully used for catalytic decomposition of methane to produce CO-free hydrogen suitable for hydrogen fuel cells. The use of nickel acetate as a nickel precursor, for the preparation of the catalysts, saves not only hydrogen (our product of interest), but also time and energy, by eliminating the pretreatment step (i.e., using H_2 at high temperature ($> 500\,^{\circ}C$) for at least 2 h). In this sense, the activity of the catalyst prepared with nickel acetate (8 and 40 wt%), supported on SiO_2 or cordierite, as prepared, was very close to the activity obtained with the catalysts prepared with nickel nitrate (pre-reduced with H_2). These catalysts, once deactivated by carbon deposition, were regenerated with steam at 600 °C. The steam regeneration produced additional H_2 and preserved nickel in the metallic form.

(2) The use of nickel acetate as the catalyst's nickel precursor led to materials with a higher surface area than those obtained when nickel nitrate was used, regardless of the type of support (SiO_2 or cordierite).

(3) The NiO mean crystallite size could be varied by a change in (1) the nickel percentage weight, (2) the type of gas used during calcination (air or nitrogen), and (3) the catalyst support.

(4) For catalyst supported on SiO_2 ($\sim$ 200–300 m^2/g), the carbon yield (g_C/g_{Ni}) attained during methane decomposition increased with an increase in the catalyst's NiO mean crystallite size. SiO_2 stabilized NiO particles (1.5–20 nm) during in situ reduction by methane and minimized sintering of Ni^0 particles. In contrast, cordierite could not stabilize the NiO or Ni^0 particles in the same way as SiO_2, and significant sintering of Ni^0 particles occurred.

Acknowledgment

The authors are grateful to the Connecticut Global Fuel Cell Center and the U.S. Army for financial support.

References

[1] J. Armor, Appl. Catal. Gen. 76 (1999) 159.
[2] R. Cortright, R. Davda, J. Dumesic, Nature 418 (2002) 964.
[3] T. Zhang, M. Amiridis, Appl. Catal. A: Gen. 167 (1998) 161.
[4] R. Aiello, J. Fiscus, H. Loye, M. Amiridis, Appl. Catal. A: Gen. 192 (2000) 227.
[5] A. Diks, J. Power Source 61 (1996) 113.
[6] M. Matsukata, T. Matsushita, K. Ueyama, Chem. Eng. Sci. 51 (1996) 2769.
[7] M. Ermakova, D. Ermakov, G. Kuvshinov, L. Plyasova, J. Catal. 187 (1999) 77–84.
[8] J.-W. Snoeck, G. Froment, M. Fowles, J. Catal. 169 (1997) 240–249.
[9] S. Takenaka, S. Kobayashi, H. Ogihara, K. Otsuka, J. Catal. 217 (2003) 79–87.
[10] S. Takenaka, Y. Shigeta, E. Tanabe, K. Otsuka, J. Catal. 220 (2003) 468–477.
[11] V. Choudhary, S. Banerjee, A. Rajput, J. Catal. 198 (2001) 136.
[12] V. Choudhary, S. Banerjee, A. Rajput Appl. Catal. A: Gen. 234 (2002) 259.
[13] T. Choudhary, C. Sivadinarayana, C. Chusuei, A. Klinghoffer, D. Goodman, J. Catal. 199 (2001) 9–18.
[14] P. Gronchi, P. Kaddouri, P. Centola, R. Del Rosso, J. Sol–Gel Sci. Technol. 26 (2003) 843.
[15] V. Recupero, L. Pino, R. Di Leonardo, M. Lagana, G. Maggio, J. Power Source 71 (1998) 208.
[16] A. Da Silva, M. De Moura, L. Mercuri, A. Santo, J. Matos, An. Assoc. Bras. Quim. 47 (1998) 133.
[17] M. Elmasry, A. Gaber, E. Khater, J. Therm. Anal. Cal. 47 (1996) 757.
[18] G. Hussein, A. Nohman, K. Attyia, J. Therm. Anal. Cal. 42 (1994) 1155.
[19] M. Mohamed, S. Halawy, M. Ebrahim, J. Anal. Appl. Pyrol. 27 (1993) 109.
[20] A. Gadalla, H. Yu, Thermochim. Acta 164 (1990) 21.
[21] A. Galwey, S. McKee, T. Mitchell, M. Brown, A. Bean, React. Solid. 6 (1988) 173.

[22] W. Pease, R. Segall, R. Smart, P. Turner, J. Chem. Soc. Faraday Trans. 82 (1986) 747.
[23] J. Doremieux, Compt. Rend. 261 (1965) 4426.
[24] J. Leicester, M. Redman, J. Appl. Chem. 12 (1962) 357.
[25] V.Yu. Bychkov, O.V. Krylov, V.N. Korchak, Kinet. Catal. 43 (1) (2002) 94.
[26] K. Otsuka, Q. Lin, A. Morikawa, Inorg. Chim. Acta 118 (1986) L23.
[27] R.K. Ungar, X. Zhang, R.M. Lambert, Appl. Catal. 42 (1988) L1.
[28] A. Slagtern, Y. Schuurman, C. Leclercq, X. Verykios, C. Mirodatos, J. Catal. 172 (1997) 118.
[29] S. Takenaka, H. Ogihara, K. Otsuka, J. Catal. 208 (2002) 53.